IL NUOVO CIMENTO Vol. 37 C, N. 6 Novembre-Dicembre 2014
DOI 10.1393/ncc/i2015-11837-2

Colloquia: LaThuile14

Recent results from the Daya Bay experiment

V. Pěč on behalf of the Daya Bay Collaboration

Charles University in Prague, Faculty of Mathematics and Physics
Institute of Particle and Nuclear Physics, V Holešovičkách 2
180 00 Prague, Czech Republic

ricevuto il 31 Luglio 2014

Summary. — The Daya Bay experiment was designed to measure the least known mixing angle in the three-flavor neutrino mixing framework, θ_{13}, with unprecedented precision by employing a relative rate measurement of electron antineutrinos from nuclear reactors. Data collected in a 217 day long period when six detectors were operational have been analyzed. Rate and energy spectra analysis yielded $\sin^2 2\theta_{13} = 0.090^{+0.008}_{-0.009}$, as well as a new result for an effective mass squared splitting $\Delta m^2_{ee} = 2.59^{+0.19}_{-0.20} \times 10^{-3}\,\mathrm{eV}^2$. The experiment started taking data in its full configuration with 8 detectors operational in fall 2012. We will briefly describe the experiment and the recent results. We will also overview future prospects of the experiment.

PACS 12.15.Ff – Quark and lepton masses and mixing.
PACS 14.60.Pq – Neutrino mass and mixing.

1. – Introduction

Development in neutrino physics in the past decade led naturally to the need of precision measurements of parameters of the phenomenological model of neutrino flavor oscillations. In the framework of 3 neutrinos mixing the mixing parameter θ_{13} has an important role. It's non-zero value is a necessary condition for CP violation in the lepton sector. Non-ambiguous measurements of θ_{13} can be achieved by studying disappearance of electron antineutrinos from nuclear reactors.

The survival probability of reactor electron antineutrino with energy E after traveling distance L from its source is expressed by

$$P_{\bar{\nu}_e \to \bar{\nu}_e}(L) = 1 - \sin^2 2\theta_{13} \sin^2\left(\frac{\Delta m^2_{ee} L}{4E}\right) - \cos^4\theta_{13} \sin^2 2\theta_{12} \sin^2\left(\frac{\Delta m^2_{21} L}{4E}\right), \tag{1}$$

© Società Italiana di Fisica

where we defined an effective mass squared splitting Δm^2_{ee} so that $\sin^2\left(\frac{\Delta m^2_{ee}L}{4E}\right) = \cos^2\theta_{12}\sin^2\left(\frac{\Delta m^2_{31}L}{4E}\right)+\sin^2\theta_{12}\sin^2\left(\frac{\Delta m^2_{32}L}{4E}\right)$. $\Delta m^2_{ij} = m^2_i - m^2_j$ is the difference in masses squared of neutrino mass eigenstates. For the current values of oscillation parameters and for the energy range relevant for reactor antineutrino measurements, Δm^2_{ee} does not, in a good approximation, depend on energy E.

Daya Bay experiment presented two precise measurements in the past [1,2] where both used only neutrino signal rate from each detector to determine the mixing parameter θ_{13}. This paper describes a method which uses also shape of the energy spectrum in addition to the rate [3]. This method improves sensitivity of the $\sin^2 2\theta_{13}$ measurement and allows a determination of Δm^2_{ee} introduced in eq. (1).

In the following, I will briefly describe the experiment, summarize some aspects of energy reconstruction, and present the analysis method and its results. At the end of the paper I will overview the future prospects of the Daya Bay experiment and will briefly summarize.

2. – Detector description

The Daya Bay experiment is located at the Daya Bay nuclear power plant complex on the south-east coast of China. Electron antineutrinos are produced in the cores of three pairs of nuclear reactors, Daya Bay, Ling Ao, and Ling Ao-II, with maximal thermal power of 17.4 $\mathrm{GW_{th}}$ in total. They are detected with detectors placed in experimental halls at two near sites, Daya Bay and Ling Ao, and one far site. The far site is about 1900 m and 1500 m away from the Daya Bay and Ling Ao power plants, respectively. The distances were chosen so that the far experimental hall would be near the first oscillation minimum of the probability in eq. (1). All three halls are situated underground with adequate shielding against cosmic rays.

The antineutrinos interact through the inverse beta decay (IBD), $\bar{\nu}_e + p \to n + e^+$. This reaction produces two successive signals. The prompt from the positron energy loss and annihilation. The delayed from gammas from the neutron capture.

The Daya Bay antineutrino detector is a 5 m by 5 m cylindrical stainless steel vessel which consists of three nested cylindrical zones partitioned with two cylindrical acrylic tanks. The innermost region is filled with gadolinium-loaded organic liquid scintillator. This volume serves as the antineutrino target and mean capture time of $\sim 30\,\mu$s for neutrons in the target is due to high capture cross-section of gadolinium. The middle layer is filled with liquid scintillator to aid detection of gammas that escape from the target volume. The scintillation light produced in the active volume is detected by 192 8-inch photomultiplier tubes (PMT) mounted on the inner side of the steel tank. The layer between the steel tank and the outer acrylic vessel is filled with transparent mineral oil. The target region and the middle layer of scintillator weigh about 20 ton each, and have diameter and height of 3 m and 4 m, respectively. There are 2 detectors at each of the near sites and 4 at the far site.

The detectors at each experimental hall are placed inside water pools. The water pool serves as an effective shielding against radioactivity from the surrounding rock and against neutrons produced in the rock by cosmogenic muons. The pools are divided into two optically separated regions, inner water shield and outer water shield, each of which is instrumented with PMTs and works as an independent Čerenkov detector of cosmic ray muons. The pools are covered with multi-layered resistive plate chambers.

Detailed description of the detectors and their performance can be found in [4].

3. – Detector energy response

Precise knowledge of the energy response of the detectors is crucial in the oscillation analysis as it determines uncertainties of event selection efficiencies and uncertainties in comparisons of spectral shapes from each hall. Therefore, attention was paid to proper energy calibration, and estimation of non-linear response of the detectors.

Three calibration units are mounted on top of each detector. Each unit has LED, a ^{68}Ge source, and a combined source of ^{241}Am-^{13}C and ^{60}Co. The sources can be vertically positioned inside the detector along 3 axes, one in the center of the detector, one by the edge of the target region, and one in the middle layer. The LED source allows to calibrate PMT gains, ^{68}Ge, ^{241}Am-^{13}C, and ^{60}Co serves as anchors for energy calibration and for determination of non-linear response of the detector. The sources are regularly lowered into the detectors during calibration runs. In addition to regular calibration we performed special calibration runs during installation works in summer 2012 with additional sources (^{137}Cs, ^{54}Mn, ^{40}K, ^{241}Am-^{9}Be, and Pu-^{13}C) deployed in detectors in Daya Bay near hall.

Detector energy response has been studied extensively and an empirical model was constructed which takes into account scintillation quenching, Čerenkov radiation contribution, and non-linear effects of the readout electronics. The treatment is divided into two parts, the first part determines the non-linear response of the liquid scintillator, which is particle dependent, the second one determines effects of readout electronics charge collection due to the time profile of the incoming signal (scintillator, PMT shaping, etc.). Regular and the special calibration sources together with natural radioactive elements, ^{40}K and ^{208}Tl, and cosmic-ray-induced ^{12}B are used to constrain the energy model. Geant4-based Monte Carlo simulation is used to correlate e^- scintillator non-linearity to response to γ and e^+.

The resulting energy model is shown in fig. 1, together with a plot of ratios of the reconstructed to expected energies for various sources, and with measured energy spectrum of ^{12}B decays.

Absolute energy scale uncertainty was determined to be within 1.5% in the energy range of interest, based on comparisons of concurrent energy models. We estimated the relative uncertainty to be 0.35% based on differences in reconstructed energies for selected sources.

4. – Analysis

The $\bar{\nu}_e$ interaction events are identified in the data as follows. Signals caused by spontaneous light emission from the PMTs are identified and removed from the sample. Coincident signals are selected if the prompt signal has reconstructed energy in the interval 0.7–12 MeV and the delayed signal has energy reconstructed in the interval 6–12 MeV. The time interval between the two must be longer than 1 μs and shorter than 200 μs. In order to avoid ambiguity in the selection of the prompt and delayed signals when there are more choices for the specified time window we require no other prompt-like signal in 400 μs before the delayed signal and no other delayed-like signals 200 μs after the delayed signal. We call this requirement a multiplicity cut.

Three types of muon veto are applied off-line. First, the $\bar{\nu}_e$ candidates are rejected if their delayed signal happened in the time interval ($-2\,\mu$s, 600 μs) with respect to a water pool muon. The water pool muon is defined as any event in either inner or outer water shield with at least 12 PMTs hit. Second, the $\bar{\nu}_e$ candidates are also rejected if

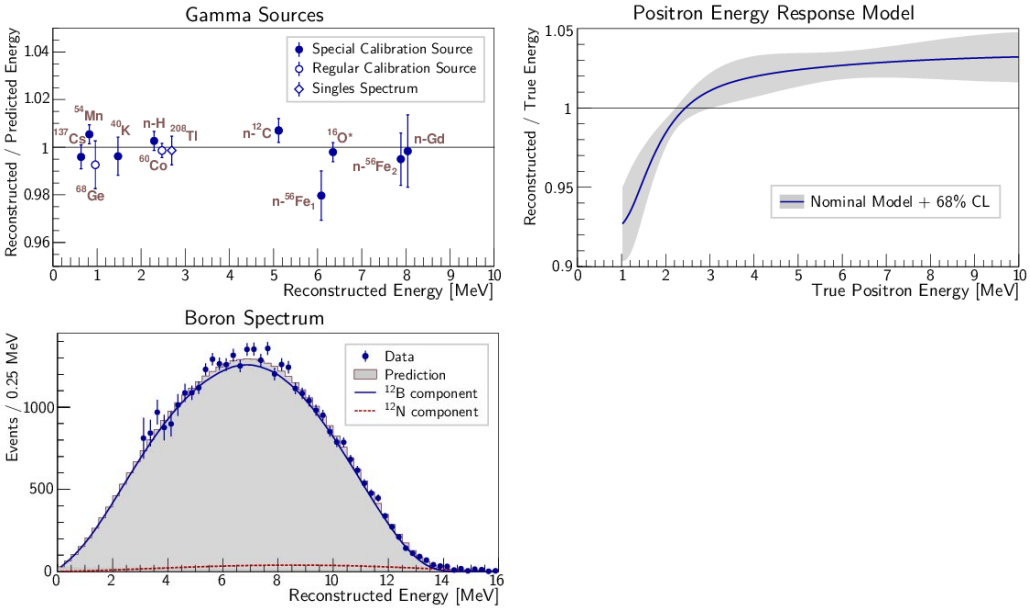

Fig. 1. – Model of non-linear energy response to positrons, top right. Various gamma sources and ^{12}B β-decay spectrum, top and bottom left, were used to constrain our energy response model, which is based on scintillation quenching, Čerenkov radiation contribution, and effects of readout electronics.

they occur within 1 ms after a muon in an antineutrino detector, identified as an event with reconstructed energy larger than 20 MeV. Third, the veto time window is extended to 1 s if the reconstructed energy in the detector is larger than 2.5 GeV, corresponding to a showering muon.

Apart from the neutrons from interactions in the target region, some neutrons from the middle layer can penetrate into the gadolinium-doped scintillator and add to the neutrino candidate sample. Part of neutrons from the $\bar{\nu}_e$ interaction in the target region may not be captured by gadolinium. Both effects were calculated using MC simulation. Efficiencies of the multiplicity cut and muon veto are directly calculated from the data with negligible uncertainty. Efficiencies of the prompt and delayed energy cuts, as well as the capture time cut were calculated based on MC simulations. Their uncertainties correlated and uncorrelated among the detectors were evaluated. However, only uncorrelated uncertainties were considered in the analysis.

Details on the efficiencies and their uncertainties can be found in [2] and [3]. Dominant contributions to the uncertainties in rate and shape analysis come from the delayed energy cut efficiency, 0.12%, gadolinium capture fraction, $< 0.1\%$, and relative energy scale differences, 0.35%.

5. – Backgrounds

The major backgrounds in the $\bar{\nu}_e$ measurement are accidental coincidences of otherwise uncorrelated events and decays of ^{9}Li/^{8}He isotopes. The isotopes are produced in interactions of cosmic rays in the detector and a fraction of them undergo beta decay with emission of a neutron creating IBD-like signal. Due to their relatively long lifetime,

TABLE I. – *Summary of total statistics of inverse β-decays (IBD) registered, the corresponding detector live time (DAQ l.t., in days), as well as significant contributors to the background of the IBD signal. The signal and background rates are corrected for efficiency of muon veto and multiplicity cuts, ϵ_μ and ϵ_m, respectively. All rates are per day and per antineutrino detector.*

	AD1	AD2	AD3	AD4	AD5	AD6
IBD	101290	102519	92912	13964	13894	13731
DAQ l.t.	191.001		189.645		189.779	
Eff. $\epsilon_\mu \cdot \epsilon_m$	0.7957	0.7927	0.8282	0.9577	0.9568	0.9566
acc.	9.54 ± 0.03	9.36 ± 0.03	7.44 ± 0.02	2.96 ± 0.01	2.92 ± 0.01	2.87 ± 0.01
fast-n	0.92 ± 0.46		0.62 ± 0.31		0.04 ± 0.02	
^{9}Li/^{8}He	2.40 ± 0.86		1.2 ± 0.63		0.22 ± 0.06	
Am-C			0.26 ± 0.12			
^{13}C$(\alpha, \mathrm{n})^{16}$O	0.08 ± 0.04	0.08 ± 0.04	0.07 ± 0.04	0.05 ± 0.03	0.04 ± 0.02	0.04 ± 0.02
IBD rate	653.3 ± 2.3	664.2 ± 2.3	582.0 ± 2.1	73.3 ± 0.66	73.03 ± 0.66	72.20 ± 0.66

they are more difficult to remove by application of veto after the corresponding muon. There is also a significant contribution to the background from one of the regular calibration sources, Am-C. Its contribution was substantial specifically in the far hall, where the signal rate is much smaller. The sources were removed from two off-axis calibration units of the detectors in the far hall during the 2012 summer installation period.

Another background accounted for are fast neutrons and $^{13}\mathrm{C}(\alpha, \mathrm{n})^{16}\mathrm{O}$ interactions. Fast neutrons are produced by the cosmogenic muons outside the detector but have enough energy to travel inside and mimic prompt and delayed coincident signal. The $^{13}\mathrm{C}(\alpha, \mathrm{n})^{16}\mathrm{O}$ are interactions initiated by the natural radioactivity inside the detector. The contributions to the backgrounds together with the $\bar{\nu}_e$ rates are shown in table I. Due to the relatively low level of the backgrounds, their respective uncertainties do not significantly affect the final result's systematic uncertainty.

6. – Result

Previously [1, 2], we determined the mixing parameter θ_{13} from the comparison of the $\bar{\nu}_e$ rates at the far and the near sites. Current analyses take into account also the shape of the measured signal energy spectra at each site. This approach slightly reduces systematic uncertainty in the θ_{13} measurement and it allows measurement of the relevant mass squared splitting.

We constructed a binned log-likelihood statistics from background-subtracted data with nuisance parameters for detector energy response, backgrounds, and reactor flux model, constrained by penalty terms. In the prediction of $\bar{\nu}_e$ rate, we used the following constrained oscillation parameters, $\sin^2 2\theta_{12} = 0.857 \pm 0.024$ and $\Delta m^2_{21} = (7.50 \pm 0.20) \times 10^{-5}\,\mathrm{eV}^2$. The best-fit values are $\sin^2 2\theta_{13} = 0.090^{+0.008}_{-0.009}$ and $|\Delta m^2_{ee}| = (2.59^{+0.19}_{-0.20}) \times 10^{-3}\,\mathrm{eV}^2$ with $\chi^2/\mathrm{NDF} = 163/153$ (errors are 68.3% confidence level (C.L.) intervals). The 68.3%, 95.5%, and 99.7% C.L. allowed regions in the $|\Delta m^2_{ee}|$ *vs.* $\sin^2 2\theta_{13}$ plane are

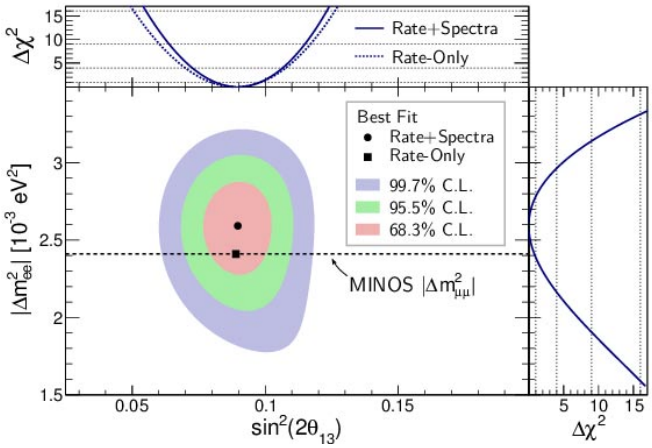

Fig. 2. – 1-, 2-, and 3-σ equivalent confidence level contours in the parameter space of the two measured oscillation parameters. $\Delta\chi^2$ projections are also shown for the combined analysis and compared to $\Delta\chi^2$ curve of the rate-only analysis [2]. MINOS measured value of the mass-square splitting [5] is also shown for reference.

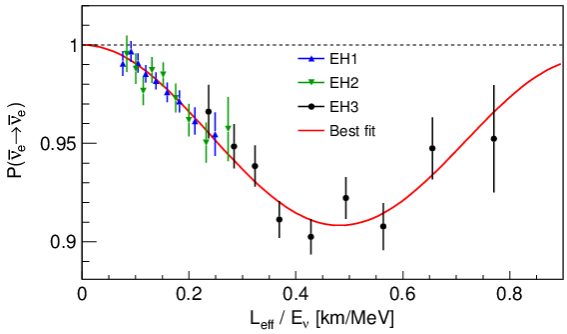

Fig. 3. – Measured spectral distortions due to $\bar{\nu}_e$ oscillations expressed as L/E dependent oscillation probability. Measured spectra from all 3 halls are used. Best-fit oscillation curve is also shown.

shown in fig. 2. The result is consistent with $|\Delta m^2_{32}| = (2.37^{+0.09}_{-0.09}) \times 10^{-3}\,\mathrm{eV}^2$(1) as measured via ν_μ and $\bar{\nu}_\mu$ disappearance [5].

The uncertainty in determination of both parameters is dominated by statistics. Most prominent contributions to the systematic uncertainties of $\sin^2 2\theta_{13}$ are related to reactor neutrino flux, relative detector efficiencies, and relative energy scale. The latter two contributors play dominant role also in the estimation of Δm^2_{ee}.

We re-expressed measured positron energy spectrum as the electron antineutrino survival probability *versus* propagation distance L over antineutrino energy E_ν. We obtained the effective baseline L_{eff} equating the calculated oscillated flux for the complex geometry with a simple single source calculation. The data points are calculated as the best-fit oscillation probability normalized by ratio of the measured to expected number of events in the respective bin [3]. The nearly complete oscillation cycle can be seen on fig. 3.

(1) For normal mass hierarchy.

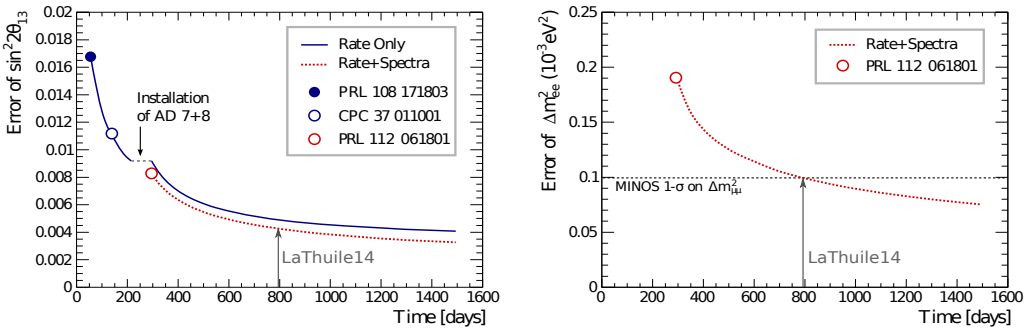

Fig. 4. – The evolution of Daya Bay sensitivities of the errors of $\sin^2 2\theta_{13}$ (left) and $|\Delta m^2_{ee}|$ (right) as predicted assuming no improvement of the systematic uncertainties. Current sensitivity of MINOS experiment [5] is also plotted for reference. Date of the conference is indicated for viewer's convenience.

7. – Prospects

On October 19, 2012, the experiment started taking data in the full configuration with 8 antineutrino detectors placed in the three experimental halls. While the uncertainty of the current results is still dominated by the statistics, with 3 years of data taking the systematic uncertainty will dominate. See fig. 4 for the predicted sensitivity to the two parameters assuming no improvement in the systematic uncertainties.

An oscillation analysis of events with neutrons captured on hydrogen instead of gadolinium is currently ongoing. It provides largely independent measurement of the $\bar{\nu}_e$ oscillations and combined analysis will further increase precision of the measurement.

With high statistics collected, Daya Bay will also give precise measurement of the energy spectrum and total flux of the reactor antineutrinos.

8. – Summary

The Daya Bay Experiment gave most precise measurement of $\sin^2 2\theta_{13}$ using its full 6-antineutrino-detector period which spanned over a period of about 190 live days and yielded nearly 340000 neutrino events. The spectral shape and rate analysis provided improved sensitivity to $\sin^2 2\theta_{13}$ and allowed measurement of Δm^2_{ee} with precision competitive with measurements of $\Delta m^2_{\mu\mu}$ by accelerator experiments. During the analysis our energy model has been improved significantly. With further improvements of the model and the knowledge of absolute detection efficiency Daya Bay will provide high-statistics measurement of the absolute flux and energy spectrum of the reactor $\bar{\nu}_e$.

* * *

The Daya Bay Experiment is supported in part by the Ministry of Science and Technology of China, the United States Department of Energy, the Chinese Academy of Sciences, the National Natural Science Foundation of China, the Guangdong provincial government, the Shenzhen municipal government, the China Guangdong Nuclear Power Group, Shanghai Laboratory for Particle Physics and Cosmology, the Research Grants Council of the Hong Kong Special Administrative Region of China, University Development Fund of The University of Hong Kong, the MOE program for Research of Excellence at National Taiwan University, National Chiao-Tung University, and NSC

fund support from Taiwan, the U.S. National Science Foundation, the Alfred P. Sloan Foundation, the Ministry of Education, Youth and Sports of the Czech Republic (project No. LH14290), Yale University, the Joint Institute of Nuclear Research in Dubna, Russia, and the CNFC-RFBR joint research program. We acknowledge Yellow River Engineering Consulting Co., Ltd. and China railway 15th Bureau Group Co., Ltd. for building the underground laboratory. We are grateful for the ongoing cooperation from the China Guangdong Nuclear Power Group and China Light & Power Company.

REFERENCES

[1] An F. P. *et al.* (Daya Bay Collaboration), *Phys. Rev. Lett.*, **108** (2012) 171803.
[2] An F. P. *et al.* (Daya Bay Collaboration), *Chin. Phys. C*, **37** (2013) 011001.
[3] An F. P. *et al.* (Daya Bay Collaboration), *Phys. Rev. Lett.*, **112** (2014) 061801.
[4] An F. P. *et al.* (Daya Bay Collaboration), *Nucl. Instrum. Methods A*, **685** (2012) 78.
[5] Coelho J. A. B. (for the MINOS Collaboration), *Results and prospects from MINOS and MINOS+*, NuFACT, 2013.